Structural and Magnetic Properties of Barium-Strontium-Hexaferrite Material $Ba_{0.6}Sr_{0.4}Fe_{10-x}Co_xMnTiO_{19}$ (x = 0.5; 1.0; and 1.5) as Microwave Absorbers

Yohanes Edi Gunanto[1,*], Maykel Manawan[2], Maya Puspitasari Izaak[1], Henni Sitompul[1], Yunasfi[3] & Wisnu Ari Adi[3]

[1]Faculty of Education, Universitas Pelita Harapan, Jalan M.H. Thamrin, Karawaci, Tangerang, 15811, Indonesia
[2]Teknologi Daya Gerak, Universitas Pertahanan Indonesia, Jalan Anyar, Kompleks IPSC Sentul, Bogor 16810, Indonesia
[3]Research Center for Advanced Materials, Building 440, BRIN, Jalan Raya PUSPIPTEK, South Tangerang, 15314, Indonesia
*E-mail: yohanes.gunanto@uph.edu

Abstract. We discuss the structure properties of $Ba_{0.6}Sr_{0.4}Fe_{10-x}Co_xMnTiO_{19}$(BSFCMTO) for x = 0.5, 1.0, and 1.5 that influence its magnetic properties as a microwave absorber. A solid-state reaction method using high-energy milling was used to synthesize hexaferrite. There were no structural changes when the Co^{2+} ion was substituted for the Fe^{3+} ion; the structures of all samples were hexagonal and the space group was P63/mmc. The surface morphology had heterogeneous particles with a size of 300 to 600 nm. The magnetic properties tended to decrease with an increasing number of Co^{2+} ion substitutions. The reflection loss (RL) had a minimum value of -14.89 dB. This value was reached at a frequency of 10.96 GHz and had a bandwidth at 1.24 GHz with a sample thickness of 1 mm in the $Ba_{0.6}Sr_{0.4}Fe_{9.9}Co_{0.1}MnTiO_{19}$ sample.

Keywords: *absorbent; barium-strontium-hexaferrite; cobalt-substitution; microwave; milling.*

1 Introduction

Ferrite material, particularly M-type hexaferrite with the general formula $MFe_{12}O_{19}$ (M = Ba, Sr, or a Ba-Sr combination), is still attractive to many researchers because it is very applicable. At low frequencies, it has a high dielectric constant and a low dielectric loss tangent, so it is applicable in the radio frequency range [1] and as a microwave absorber [2,3]. For a microwave-absorbent material, two conditions must be met. Firstly, it must have the same intrinsic impedance value as the vacuum, and secondly, it must have a high dielectric constant in order to weaken the interaction between the incoming electromagnetic energy and the material [4]. Thus, the microwave absorbing material must be in the medium-hard magnetic phase. An important parameter

Received April 29th, 2023, Revised August 23th, 2023, Accepted for publication March 13th, 2024
 ISSN: 2337-5760, DOI: 10.5614/j.math.fund.sci.2024.55.3.1

for determining the size of the absorption ability is the reflection loss (RL) value of the absorbent material. The greater the value of reflection loss (negative value) as a function of frequency, the greater the ability to absorb microwaves of the material. Meanwhile, if the RL value = 0, it means that the material perfectly reflects the microwaves.

M-type hexaferrite, especially $BaFe_{12}O_{19}$, is a hard magnetic material, has high magnetic saturation, and a large coercivity field [5,6], so it is suitable to be applied as a permanent magnet [7]. To be able to be used as a microwave absorber, it needs to be engineered so that it still has high magnetic saturation while the coercivity field decreases so that it is in the medium-hard magnetic phase. Therefore, to increase the ability to absorb microwaves, substitutions can be carried out either on Ba [2], Fe [8], or simultaneously on Ba and Fe [3,4]. The Ti^{4+} ion substitution in the Fe^{3+} ion sample $Ba_{0.6}Sr_{0.4}Fe_{12-x}Ti_xO_{19}$ has a reflection loss (RL) of ~-25 dB for the value of x = 1 [3]. If the Mn^{2+} ions are substituted for the Fe^{3+} ions, the reflection loss is about -10 dB [4].

Handoko *et al.* [9] obtained values of RL ~-12.67 dB and -15.49 dB by substituting Co^{2+} and Zn^{2+} ions for Fe^{3+} ions, while Alam *et al.* [10] used Zn^{2+}, Co^{2+}, and Zr^{4+} ions to substitute the Fe^{3+} ions ($BaZn_{0.5}Co_{0.5}ZrFe_{10}O_{19}$) to obtain an RLof ~-14 dB with a sample thickness of 2.8 mm. Several synthesis methods can be used, such as sol-gel auto-combustion [11,12], synthesis via chemical route [13], solid-state reaction [8,14], and co-precipitation [15,16]. Of these methods, the solid-state reaction is the cheapest and most accessible.

From what was done in the present study, the magnetic saturation value of $BaFez_{12}O_{19}$ has Ms = 44.65 $emug^{-1}$ with a coercivity field Hc = 4.51 kOe [5]. For $Ba_{0.6}Sr_{0.4}Fe_{12}O_{19}$, the magnetic saturation has been shown to be Ms = 76.62 $emug^{-1}$ and it has an Hc coercivity field of 4.894 kOe with about 68% (-4.95 dB) of reflection loss (RL) [2] and is substituted for Ti^{4+} ($Ba_{0.6}Sr_{0.4}Fe_{10}Ti_2O_{19}$), RL = -20 dB with a bandwidth (BW) of 1.2 GHz for a sample thickness of 2 mm [3], which is substituted for Mn^{2+} ($Ba_{0.6}Sr_{0.4}Fe_{11}MnO_{19}$), with a value of RL = -10 dB and BW = 0 GHz [4]. The Co and Zn substitution ($BaCoZnFe_{10}O_{19}$) with a 3-mm thick sample has a minimum RL = -15.54 dB, a BW of 0.37 GHz [8], and a composition of $BaZn_{0.5}Co_{0.5}ZrFe_{10}O_{19}$, with a BW of approximately 1.8 GHz and RL = -14 dB [9].

Based on the results that were obtained, a problem still remains, namely the narrow bandwidth obtained. The bandwidth is the frequency width obtained when the RL value is below -10 dB. In addition, Co is able to increase the bandwidth of the RL value, which is very significant for certain compositions. In another study, the anisotropy constant of the structure along the c-axis will be reduced by the presence of Co ions in the hexaferrite structure [17]. Therefore, there are still

challenges in decreasing the coercive magnetic force and increasing the RL value with a wide enough bandwidth.

This paper is a continuation of our previous research on$Ba_{0.6}Sr_{0.4}Fe_{10}MnTiO_{19}$ [18,19]. In previous studies, the coercivity field of $Ba_{0.6}Sr_{0.4}Fe_{10}MnTiO_{19}$ was still very large, i.e., around 2990 Oe, producing an RL value of -8 dB with a bandwidth of 1 GHz. Thus, the substitution of Co^{2+} ions is expected to reduce the coercivity field and increase the RL value. This paper will discuss the impact of Co^{2+} ion substitution on the structure, magnetic magnitude and absorption capacity of microwaves (high RL and wide bandwidth) on BSFCMTO for x = 0.5, 1.0, and 1.5. The sample was processed using milling as part of the solid-state reaction procedure.

2 Experimental and Method

Stoichiometric calculations of raw materials such as $BaCO_3$, $SrCO_3$, Fe_2O_3, $CoCO_3$, $MnCO_3$, and TiO_2 were delivered during preparation of the $Ba_{0.6}Sr_{0.4}Fe_{10-x}Co_xMnTiO_{19}$ samples. Each of the raw materials was a product from Merck with 99% purity. This mixture of raw materials was put into a container made of stainless steel. Then, stainless-steel balls were added with the weight ratio between the material and the balls at 1: 1. The ingredients were milled for forty hours. The milling process was carried out in a wet state. Milling was carried out in stages, with every hour of milling interspersed with thirty minutes of rest. The samples were then sintered at 1000 °C for five hours. The stoichiometric calculation was based on the following reaction equation:

$$1.2BaCO_3 + 0.8SrCO_3 + (10\text{-}x)Fe_2O_3 + 2xCoCO_3 + 2MnCO_3 + 2TiO_2 \longrightarrow$$

$$2Ba_{0.6}Sr_{0.4}Fe_{10-x}Co_xMnTiO_{19}$$

The M-hexaferrite type's most crucial crystal and magnetic structure is its unit cell containing four blocks of ten oxygen layers arranged sequentially as S (spinel), R (hexagonal), S*, and R*, respectively. The S* and R* blocks have the same atomic arrangement as the S and R blocks, but the arrangement is rotated 180° around the c-axis. Four O^{2-} layers are in the S and S* blocks, each consisting of two layers. Six O^{2-} layers are in the R and R* blocks, each with three layers. In the middle layer of the R and R* blocks, one oxygen site is replaced by Ba^{2+} ions. The lattice constants of the M-hexaferrite structure have lattice lengths a = 5.89 Å and c = 23.19 Å. The arrangement of oxygen and Ba atoms with Fe is in octahedral (12k, 4f2, and 2a), tetrahedral (4f1), and trigonal bipyramidal/hexahedral sites (2b) on a closed hexagonal structure. Thus, the characteristic feature of this M-hexaferrite structure is the ratio of c/a ≈ 3.98.

A Philips PW1710 X-ray diffractometer with a wavelength of 1.5406 Å was used to characterize the formed phase, crystal structure, and lattice parameters from an angel of $2\theta = 10^o - 80^o$. A JEOL JED 2300 scanning electron microscope (SEM) was used to examine the surface morphology, including particle form and distribution. For magnetic characterization, a vibrating sample magnetometer (VSM) was utilized, capable of producing an external magnetic field as high as 15 kOe. In contrast, characterization of the capability to absorb microwaves was done using an Anritsu MS46322A vector network analyzer (VNA) in the frequency range of 8 to 12 GHz.

3 Result and Discussion

Henceforth, the $Ba_{0.6}Sr_{0.4}Fe_{(10-x)}Co_xTiMnO_{19}$ samples with x = 0.1, 0.3, and 0.5, willed be called EG-01, EG-03, and EG-05, respectively. The XRD result diffraction patterns can be seen in Figure 1. The main phase of Ba-Sr hexaferrite ($Ba_{0.6}Sr_{0.4}Fe_{(10-x)}Co_xTiMnO_{19}$) was formed and there was no visible shift in the peaks. This means that the Co^{2+} substitution can replace Fe^{3+}. Co^{2+} substitution does not cause structural changes. All samples had a hexagonal structure (P63/mmc) and contained a tiny quantity (~ 5%) of hematite phase (Fe_2O_3) represented by a peak at an angle $2\theta = 33.2^o$, according to JCPDS 85-0987 [20]. The formation of the M-type structure can be seen from the parameter ratio c/a, which is less than 3.98 [2,6,10].

Table 1 presents an overview of the refining outcomes using the Rietveld program. The volume of the cells increases with the increase in the value of Co substitution. This can be explained by the ionic radius of Co^{2+} (0.74 Å) being greater than that of Fe^{3+} (0.64 Å) [21]. There is no significant change in the crystallite size after Co substitution. The Scherrer equation in Eq. (1) was used to calculate the crystalline size [5]:

$$D = k\lambda/(\beta \cos\theta) \quad (1)$$

where D is the crystallite size, k is the Scherrer constant (= 0.89), λ is the wavelength (= 1.5406 Å), β is the Full width at half maximum (FWHM), and θ is the Bragg angle of the peak position. From the high-intensity peaks in the diffraction pattern of each sample, the crystal size ranged from 72 to 76 nm.

The surface morphologies obtained by scanning electron microscopy (SEM) with magnification at 10,000x for samples EG-01, EG-03, and EG-05 is shown in Figure 2. Heterogeneous particle shapes and sizes are evenly distributed. The particle size ranges from 300 to 600 nm. The particle diameter was compared to the current line scales to arrive at this conclusion.

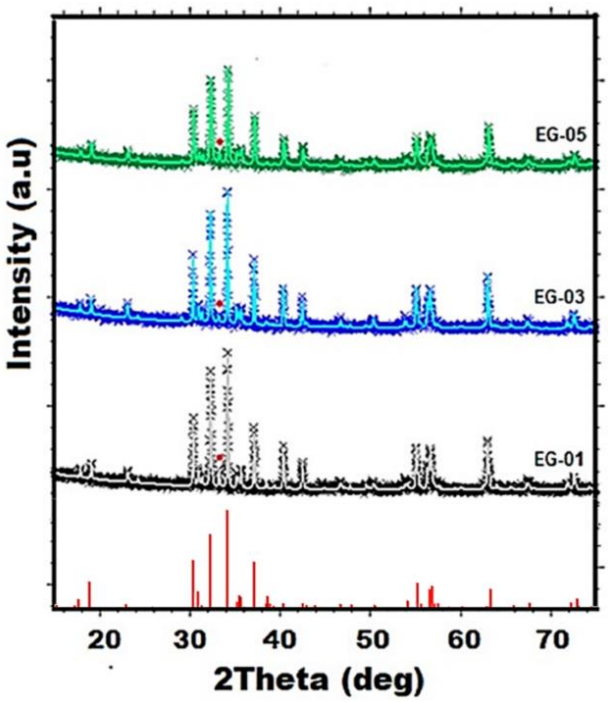

Figure 1 Rietveld refined powder XRD patterns of EG-01, EG-03, and EG-05. The red dot is the peak position of Fe_2O_3.

Table 1 Summary of the XRD refinement results with the Rietveld program.

		EG-01	**EG-03**	**EG-05**
Space group		P63/mmc	P63/mmc	P63/mmc
Cell mass		2183.15(1)	2183.15(1)	2183.15(1)
Cell volume (Å^3)		697.70(12)	698.06(6)	698.67(7)
Crystal density (g/cm^3)		5.196(1)	5.193(1)	5.189(1)
Crystallite size (nm)		72(4)	76(5)	73(5)
Lattice Parameters:	*a* (Å)	5.8967(4)	5.8986(2)	5.9005(2)
	c (Å)	23.1601(12)	23.1670(13)	23.1719(14)
	c/*a*	0.18958	0.18958	0.18958
Rexp		3.24	3.17	3.16
Rwp		3.50	3.45	3.58
GoF		1.08	1.09	1.13

There appears to be agglomeration, which is thought to be due to magnetic interactions between particles [10]. All samples can be categorized as having a single-domain-wall structure because the mean particle size was smaller than the 650 nm critical size [21]. The porosity increases as the content of Co^{2+} increases.

This is related to the crystal volume of XRD results, where the radius of the Co^{2+} ions is greater than that of the Fe^{3+} ions, causing the crystal density to decrease.

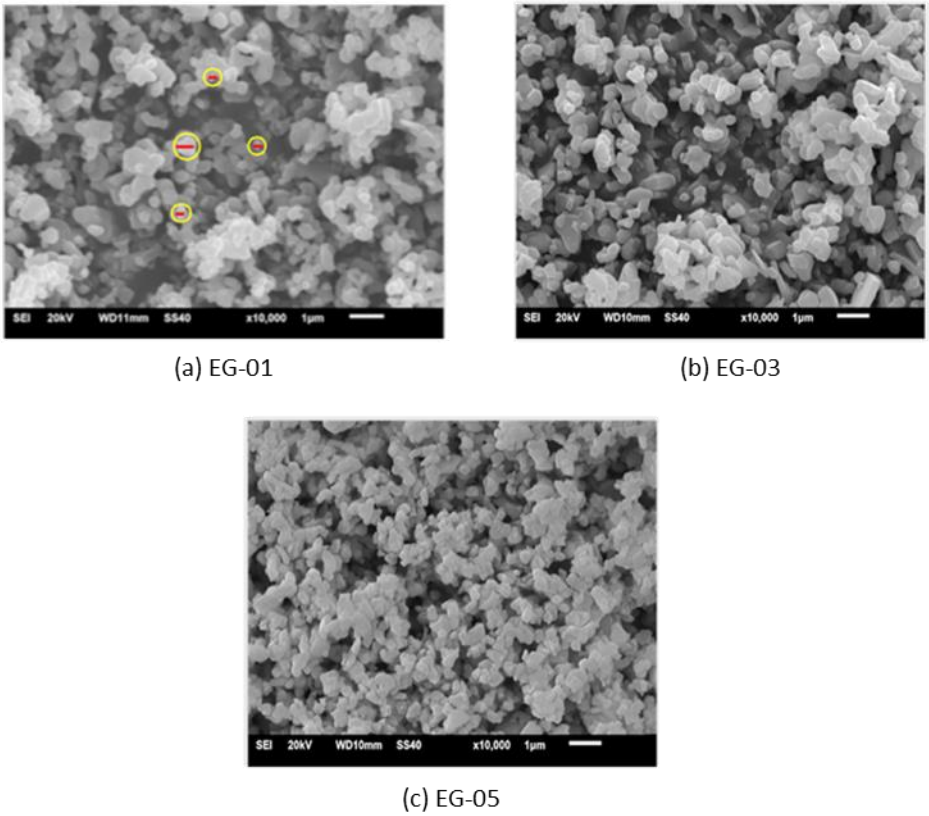

Figure 2 SEM results for samples (a) EG-01, (b) EG-03, and (3) EG-05 displaying the surface morphology.

A test on the magnetization properties was carried out at room temperature. The magnetic properties obtained in relation to the external magnetic field are represented by M-H hysteresis loops. The hysteresis curves of samples EG-01, EG-03, and EG-05 can be seen in Figure 3. The saturation, remanence, and coercivity of magnetic of all samples can be seen in Table 2. The larger cobalt Co^{2+} ion substitution reduces its magnetic magnitude, both Ms magnetic saturation, Mr magnetic remanence, and Hc coercivity. This is because the magnetic dipole moment for Co^{2+} ions (~ 3 μB) is smaller than for Fe^{3+} ions (~ 5 μB) [10, 22]. In addition, the decrease in Ms magnetic saturation is also due to the presence of the α-Fe_2O_3 phase, which is non-magnetic [21].

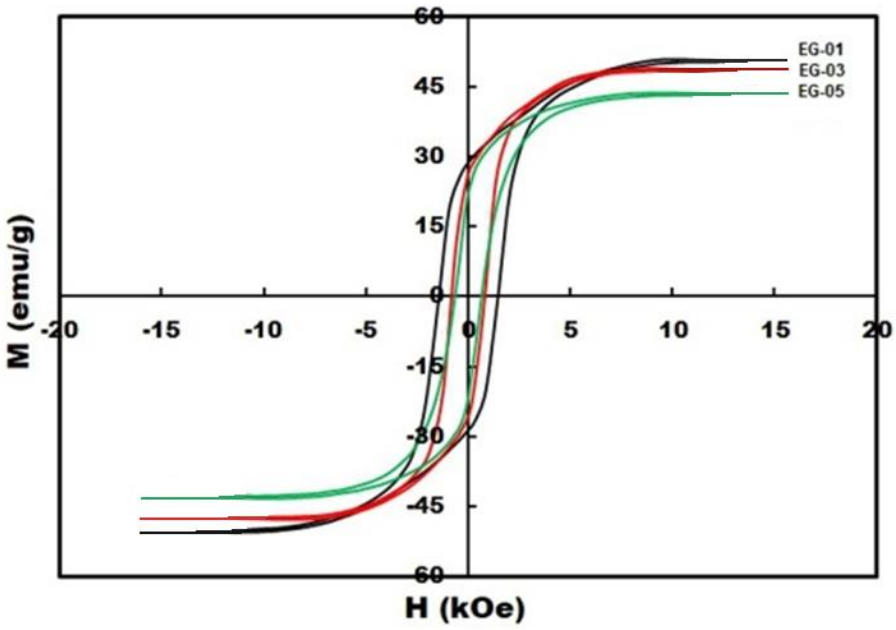

Figure 3 Magnetization hysteresis curve at room temperature for the sample $Ba_{0.6}Sr_{0.4}Fe_{(10-x)}Co_xTiMnO_{19}$ with x = 0.1 (EG-01), 0.3 (EG-03), and 0.5 (EG-05), respectively.

Table 2 Magnetic saturation and coercivity of $Ba_{0.6}Sr_{0.4}Fe_{(10-x)}Co_xTiMnO_{19}$ sample.

Sample	Ms ($emug^{-1}$)	Mr ($emug^{-1}$)	Hc (kOe)
EG-01	50.55	28.57	1.50
EG-02	48.85	26.01	1.20
EG-03	43.56	25.58	1.01

Figure 3 shows a change in magnetic properties from hard magnetic [18,19] to softer magnetic. It appears that the magnetic coercivity field changes as well as the saturation magnetization are decreasing, which shows a tendency to decrease with the rise of the concentration of Co^{2+} doping ions in the material. In this experiment, refinement of the cationic distribution was not carried out, which can determine which sites are occupied by Co^{2+} ions. However, in this case, it is assumed that Co^{2+} ions occupy a portion of all Fe^{3+} sites, so that the reduction in magnetic properties is only determined based on the reduced number of magnetic dipole moments due to differences in the Bohr magneton content between Fe^{3+} and Co^{2+}.

The role of Co^{2+} ions is thought to be able to stimulate the growth of magnetic domains. This assumption was supported based on the results of X-ray diffraction pattern analysis, which showed that the value of the c-lattice parameter appears to increase with increasing Co^{2+} ion concentration, causing a decline in the value of anisotropy along the c-axis [23-26]. The magnetic domain is an area in a magnetic material where the magnetization is uniformly oriented. This means that the individual atoms have magnetic moments in parallel with each other in the same direction.

The materials' magnetic behavior is attributed to the structure of the magnetic domain. The crystal lattice of most magnetic materials has magnetic anisotropy, meaning that they have a direction of magnetization that is easily parallel to one of the crystal axes. In order to change the magnetization of the material in another direction, additional energy is required, which is referred to as magneto crystalline anisotropy energy. Based on the characteristics of the magneto crystalline anisotropy, in M-hexagonal ferrite, the plane on the crystallographic a-b axis is the hard-axis, and the crystallographic c-axis is known as the easy-axis. The intrinsic magnetic properties of these materials are completely dependent on the distribution of cations at the crystallographic sites. That is, the intrinsic properties of the magnetic material can be adjusted by adjusting the distribution of cations at the crystallographic site.

The explanation of which site is occupied by the Co^{2+} ions in substitution to M-type hexaferrite is still subject of discussion. The presence of cations in Fe3+ ions (4f2/spin-down) results in an increase in the number of Fe^{3+} ions (spin-up), as per the results of previous studies using spin-orbit interaction (SOI) to calculate the electronic structure between Fe^{2+} ions and O^{2-} ions that form clusters [27]. Additionally, the magnetic dipole moment for Co^{2+} ions is smaller than that of Fe^{3+} ions. This ion substitution tends to be at the tetrahedral site (4f1) [27,28], thereby weakening the super-exchange interaction between the octahedral and tetrahedral sites.

The Co^{2+} ions occupy two sites, namely 2a (spin-up) and $4f_2$ (spin down) [7], while the Fe^{3+} ions in the M-type hexaferrite occupy five sites, namely 12k, 2a, and 2b (spin-up) and $4f_1$ and $4f_2$ (spin-down) [14,27,29]. The magnetic moments of ions both spinning down and spinning up at the octahedral and tetrahedral sites cause this change, which is highly dependent on the Fe^{3+}– O^{2-} – Fe^{3+} [28] super-exchange interaction. In general, the distribution of spin-up orientations is at 6 Fe^{3+} octahedral-site ions (12k and 2a) and 1 Fe^{3+} bipyramid ion (2b), while 2 Fe^{3+} ions are oriented to spin down at the tetrahedral ($4f_1$) and octahedral ($4f_2$) sites.

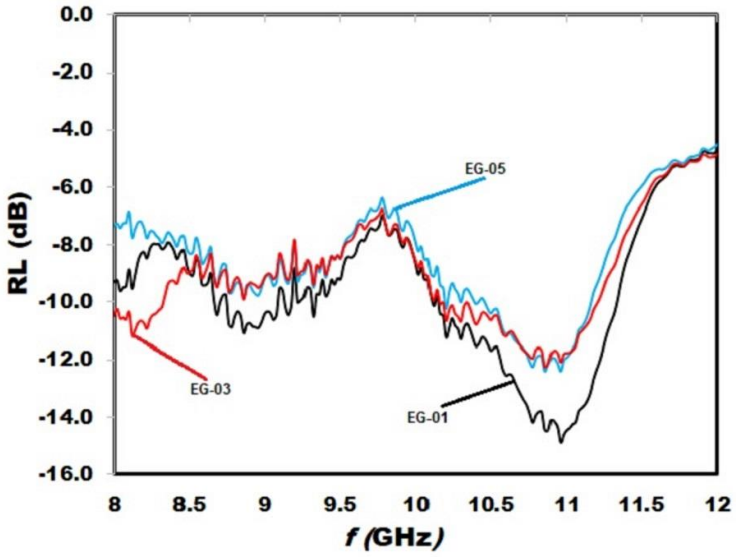

Figure 4 Frequency-dependent (f) reflection loss (RL) curves for samples EG-01, EG-03, and EG-05 at a frequency of 8 to 12 GHz.

Reflection loss (RL) is an indicator of microwave absorption. The value of RL (dB) is expressed by Eq. (2) [30]:

$$RL(dB) = 20\log|(Z_{in} - 1)/(Z_{in} + 1)| \quad (2)$$

with Z_{in} as the input impedance normalized by Eq. (3).

$$Z_{in} = {}^{Z_i}/_{Z_o} = \sqrt{\frac{\mu_r}{\varepsilon_r}}\tanh\left(\frac{j2\pi\sqrt{\mu_r\varepsilon_r}}{c}fd\right) \quad (3)$$

Where Z_i represents the input impedance, Z_o the impedance of free space, d the thickness of the absorber, μ_r the relative permeability, ε_r the relative permittivity of the medium, and f and c the frequency and velocity of electromagnetic waves in a vacuum, respectively. If $Z_i = Z_0$, then there will be an ideal condition because the microwaves are completely absorbed.

The frequency-dependent reflection loss (RL) for samples EG-01, EG-03, and EG-05 in the frequency range of 8 to 12 GHz is shown in Figure 4. In Table 3, the VNA measurement results for a sample thickness of 1 mm are written in detail. The best results were obtained for the EG-01 sample with a minimum RL value of -14.89 dB at a frequency of 10.96 GHz and a bandwidth of 1.24 GHz. The results with this Co^{2+} ion substitution were better than those obtained

previously, with a sample thickness of 2 mm and a particle size of 20 to 30 nm for a silicon rubber composite with 20% $Ba_{0.6}Sr_{0.4}Fe_{10}MnTiO_{19}$ filler, i.e., RL = -15 dB, 1 GHz bandwidth [31]. The results obtained by a larger bandwidth (Sözeri *et al.* [32]), amounted to 4 GHz, but the value of RL was ~-10 dB with a sample thickness of 2 mm for the $BaFe_{10}MnTiO_{19}$ sample. The thickness of the sample influenced the RL value during the test and the processing temperature sintering of the material. A sample thickness of 2 mm and a sintering temperature of 800 °C, $BaFe_{10}CoNiO_{19}$, RL = -14.47 dB, was better than a sintering temperature of 600°C, RL = - 12 dB [33]. Thus, several factors affect the RL value, namely composition, sample thickness, and sintering temperature, which affect the particle size. It is known that the EG-01 sample with a thickness of 1 mm had better absorption compared to the results obtained from previous studies, which had a thickness of 2 mm. According to Eqs. (2) and (3), the absorption of microwaves is proportional to the thickness of the sample. However, in this study, it was found that with a thinner thickness, a higher absorption was able to be produced.

Table 3 Summary of microwave absorption result in the 8 to 12 GHz frequency range.

Sample	RL (dB)	f (GHz)	BW (GHz)
EG-01	-14.89	10.96	1.24 (-10 dB)
EG-03	-12.39	10.86	0.80 (-10 dB)
EG-05	-12.24	10.86	1.08 (-10 dB)

This indicates, then, that the barium hexaferrite crystal structure with a composition of x = 0.1 is the ideal composition to provide the most optimal microwave absorption when Co^{2+} ions are partially substituted for Fe^{3+} ions. This significant absorption is caused by remanent magnetization at its ideal value, a drop in the coercivity field Hc, and a decline in the anisotropic field along the c axis [25,26]. This is because the movement of the domain walls and the rotation of the magnetization and spin resonance are easier with the presence of Co^{2+} ions [23-26,28].

4 Conclusion

For x = 0.1, 0.3, and 0.5, the lattice volume rises when Co^{2+} ions are substituted for Fe^{3+} ions (BSFCMTO), but the crystal structure remains the same. Each sample is hexagonally structured and the space group is P63/mmc. Because of the substitution of Co^{2+} ions, the magnitude of magnetic saturation and remanence as well as the coercivity field was reduced. According to these results, this M-hexaferrite type can be applied as a microwave absorber. The best RL value was -14.89 dB, with the f at 10.96 GHz with a bandwidth of 1.24 GHz.

Acknowledgement

This research was funded by the Menristek-Dikti through a Higher Education Basic Research Contract for the 2021 Budget Year with the contract number: 297/LPPM-UPH/IV/2021, in accordance with the Research Grant Implementation Assignment Agreement Letter Number 1218/LL3/PG/2021, April 1, 2021, through the Primary Research Scheme for Higher Education Fiscal Year 2021.

References

[1] Marouani, Y., Massoudi, J., Noumi, M., Benali, A., Dhahri, E., Sanguino, P., Graça, M.P.F., Valente, M.A. & Costa, B.F.O., *Electrical Conductivity and Dielectric Properties of Sr Doped M-Type Barium Hexaferrite* $BaFe_{12}O_{19}$, RSC Adv., **11**(3), pp. 1531-1542, 2021.

[2] Velhal, N., Kulkarni, G., Mahadik, D., Chowdhury, P., Barshilia, H. & Puri, V., *Effect of* Ba^{2+} *Ion on Structural, Magnetic and Microwave Properties of Screen Printed* $Ba_xSr_{1-x}Fe_{12}O_{19}$ *Thick Films,* Journal of Alloys and Compounds, **682**, pp. 73-737, 2016.

[3] Gunanto, Y.E., Cahyadi, L. & Adi, W.A., *Influence of Ti Addition on the Microwave Absorbing Behavior of* $Ba_{0.6}Sr_{0.4}Fe_{12-x}Ti_xO_{19}$ *System at X-band Frequencies,* in J. Phys.: Conf. Ser., **1091**(1), 012009, 2018.

[4] Gunanto, Y.E., Jobiliong, E. & Adi, W.A., *Microwave Absorbing Properties of* $Ba_{0.6}Sr_{0.4}Fe_{12-z}Mn_zO_{19}$ *(z=0-3) Materials in X-Band Frequencies,* J. Math. Fund. Sci., **48**(1), pp. 55-65, 2016.

[5] Al Dairy, A.R., Al-Hmoud, L.A. & Khatatbeh, H.A., *Magnetic and Structural Properties of Barium Hexaferrite Nanoparticles Doped with Titanium, Symmetry*, **11**(6), 732, 2019.

[6] Godara, S.K., Dhaka, R.K., Kaur, N., Malhi, P.S., Kaur, V., Sood, A.K., Bahel, S., Bhadu, G.R., Chaudhari, J.C., Pushkarna, I. & Singh, M., *Synthesis and Characterization of Jamun Pulp based M-type Barium Hexaferrite Via Sol-Gel Auto-Combustion,* Results in Physics, **22**, 103903, 2021.

[7] de Julian Fernandez, C., Sangregorio, C., de la Figuera, J., Belec, B., Makovec, D. & Quesada, A., *Progress and Prospects of Hard Hexaferrites for Permanent Magnet Applications*, J. Phys. D: Appl. Phys. **54**(15), 153001, 2021.

[8] Gudkov, V.V., Sarychev, M.N., Zherlitsyn, S., Zhevstovskikh, I.V., Averkiev, N.S., Vinnik, D.A., Gudkova, S.A., Niewa, R., Dressel, M., Alyabyeva, L.N., Gorshunov, B.P. & Bersuker**,** I.B., *Sub-lattice of Jahn-teller Centers in Hexaferrite Crystal,* Scientific Reports, **10**(1), 7076, 2020.

[9] Handoko, E., Budi, S., Sugihartono, I., Marpaung, M.A., Jalil, Z., Taufiq, A. & Alaydrus, *M., Microwave Absorption Performance of Barium Hexaferrite Multi-Nanolayers,* Mater. Express, **10**(8), pp. 1328-1336, 2020.

[10] Alam, R.S., Moradi, M., Rostami, M., Nikmanesh, H., Moayedi, R. & Bai, Y., *Structural, Magnetic and Microwave Absorption Properties of Doped Ba-hexaferrite Nanoparticles Synthesized by Co-Precipitation Method*, Journal of Magnetism and Magnetic Materials, **381**, pp. 1-9, 2015.

[11] Almessiere, M.A., Slimani, Y., Güngünes, H., Baykal, H., Trukhanov, S.V. & Trukhanov, A.V., *Manganese/Yttrium Codoped Strontium Nanohexaferrites: Evaluation of Magnetic Susceptibility and Mossbauer Spectra*, Nanomaterials, **9**(1), 24, 2019.

[12] Gore, S.K., Jadhav, S.S., Jadhav, V.V., Patange, S.M., Naushad, Mu., Mane, R.S. & Kim, K.H., *The Structural and Magnetic Properties of Dual Phase Cobalt Ferrite*, Scientific Reports, **7**(1), 2524, 2017.

[13] Kumar, A., Verma, M.K., Singh, S., Das, T., Singh, L. & Mandal, K.D., *Electrical, Magnetic and Dielectric Properties of Cobalt-Doped Barium Hexaferrite* $BaFe_{12-x}Co_xO_{19}$ *(x = 0.0, 0.05, 0.1 and 0.2) Ceramic Prepared via a Chemical Route*, Journal of Electronic Materials, **49**(11), pp. 6436-6447, 2020.

[14] Gunanto, Y.E., Izaak, M.P., Sitompul, H. & Adi, W.A., *Reflection Loss Characteristic as Coating Thickness Function on the Microwave Absorbing Paint at a Frequency of 8-12 GHz*, in IOP Conf. Series: Materials Science and Engineering, **515**(1), 012074, 2019.

[15] Ginting, M., Sebayang, P., Rianna, M., Situmorang, M., Fujiati, H., Tetuko, A.P., Setiadi, E.A., Kurniawan, C. & Sebayang, A.M.S., *Effect of Co and Ni Additions as Doping Materials on The Micro-Structures and the Magnetic Properties of Barium Hexa-ferrites*, Case Studies in Thermal Engineering, **18**, 100589, 2020.

[16] Dudziak, S., Ryżyńska, Z., Bielan, Z., Ryl, J., Klimczuk, T. & Zielińska-Jurek, A., *Pseudo-superparamagnetic Behavior of Barium Hexaferrite Particles*, RSC Adv., **10**(3), 18784-18796, 2020.

[17] Jiang, X., Li, S., Yu, Z., Harris, V.G., Su, Z., Sun, K., Wu, C., Guo, R. & Lan, Z., *Effect of Cobalt Substitution on Magnetic Properties of* $Ba_4Ni_{2-x}Co_xFe_{36}O_{60}$ *Hexaferrite*, AIP Advances, **8**(5), 056218, 2018.

[18] Gunanto, Y.E., Cahyadi, L., and Adi, W.A., *Effect of Mn and Ti Substitution on the Reflection Loss Characteristic of Ba0. 6Sr0. 4Fe11-zMnTizO19 (z= 0, 1, 2 and 3)*, in AIP Conference Proceedings, **1725**(1), 020023, 2016.

[19] Gunanto, Y.E., Izaak, M.P., Silaban, S.S. & Adi, W.A., *Effect of Milling Time on Microwave Absorption Ability on Barium-Hexaferrite Nanoparticles*, IOP Conf. Series: Journal of Physics: Conf. Series, **1011**(1), 012058, 2018.

[20] Chavan, V.C., Shirsath, S.E., Mane, M.L., Kadam, R.H. & More, S.S., *Transformation of Hexagonal to Mixed Spinel Crystal Structure and Magnetic Properties of Co^{2+} Substituted $BaFe_{12}O_{19}$,* Journal of Magnetism and Magnetic Materials, **398**, pp.32-37, 2016.

[21] Ghezelbash, S., Yousefi, M., Hossainisadr, M. & Baghshahi, S., *Structural and Magnetic Properties of Sn^{4+} Doped Strontium Hexaferrites Prepared via Sol-Gel Auto-Combustion Method,* IEEE Transactions on Magnetics, **54**(9), pp. 1-6, 2018.

[22] Kanagesan, S., Jesurani, S., Velmurugan, R., Prabu, S. & Kalaivani. T., *Magnetic Properties of Ni-Co Doped Barium Strontium Hexaferrite,* J. Mater. Sci: Mater Electron, **23,** pp. 1575-1579, 2012.

[23] Lisjak, D., *The Influence of Magnetic Interactions and Shape Anisotropy on the Alignment and Assembly of $BaFe_{12}O_{19}$ and Er_2O_3 Nanoplates,* Mater. Chem. Phys., **148**(1-2), pp. 311-318, 2014.

[24] Choi, M., Cho, S., Song, Y., Choi, D., Park, S. & Kim, Y., *Novel Synthesizing Method of $BaFe_{12}O_{19}$ Microrod and its Superior Coercivity with Shape Anisotropy,* Mat. Lett. **139**, pp. 292-295, 2015.

[25] Mahmood, S.H., Dushaq, G.H., Bsoul, I., Awawdeh, M., Juwhari, H.K., Lahlouh, B.I. & AlDamen, M.A., *Magnetic Properties and Hyperfine Interactions in M-Type $BaFe_{12-2x}Mo_xZn_xO_{19}$ Hexaferrites,* Journal of Applied Mathematics and Physics, **2**(05), pp.77-87, 2014.

[26] Pasko, A., Mazaleyrat, F., LoBue, M., Loyau, V., Basso, V., Kupferling, M., Sasso, C.P. & Bessais, L., *Magnetic and Structural Characterization of Nanosized $BaCo_xZn_{2-x}Fe_{16}O_{27}$ Hexaferrite in the Vicinity of Spin Reorientation Transition,* Journal of Physics: conference series **303**(1), 012045, 2011.

[27] Inoue, J., Nakamura, H. & Yanagihara, H., *Local Strain Dependence of Uniaxial Magnetic Anisotropy in M-Type Ferrites,* T. Magn. Soc. Jpn. (Special Issues), **3**(1), pp.12-18, 2019.

[28] Yang, Z., Wang, C.S., Li, X.H. & Zeng, H.X., *(Zn, Ni, Ti) Substituted Barium Ferrite Particles with Improved Temperature Coefficient of Coercivity,* J. Mater. Sci. Eng., 90(1-2), pp.142-145, 2002.

[29] Ghzaiel, T.B., Dhaoui, W., Pasko, A. & Mazaleyrat, *F., Effect of Non-Magnetic and Magnetic Trivalent Ion Substitutions on Bam-Ferrite Properties Synthesized by Hydrothermal Method,* Journal of Alloys and Compounds, Elsevier, **671**, pp. 245-253, 2016.

[30] Ibrahim, I. R., Matori, K.A., Ismail, I., Awang, Z., Rusly, S.N.A., Nazlan, R., Idris, F.M., Zulkimi, M.M.M., Abdullah, N.H., Mustaffa, M.S., Shafiee, F.N. & Ertugrul, M., *A Study on Microwave Absorption Properties of Carbon Black and $Ni_{0.6}Zn_{0.4}Fe_2O_4$ Nanocomposites by Tuning the Matching-Absorbing Layer Structures,* Scientific Reports, **10**(1), 3135, 2020.

[31] Gunanto, Y.E., Izaak, M.P., Silaban, S.S. & Adi, W.A., *Synthesis and Characterization of Barium-Hexaferrite-Based Nanocomposite on X-band Microwave,* in IOP Conf. Series: Materials Science and Engineering, **367**(1), 012040, 2018.

[32] Sözeri, H., Deligöz, H., Kavas, H. & Baykal, *A., Magnetic, Dielectric and Microwave Properties of M-Ti Substituted Barium Hexaferrites (M = M = Mn^{2+}, Co^{2+}, Cu^{2+}, Ni^{2+}, Zn^{2+}),* Ceramics International, **40**(6), pp. 8645-8657, 2014.

[33] Susilawati, Doyan, A., Khair, H., Taufik, M. & Wahyudi., *Electrical, Magnetic and Microwave Absorption Properties of M-type Barium Hexaferrites ($BaFe_{12-2x}Co_xNi_xO_{19}$),* in IOP Conf. Series: Journal of Physics: Conf. Series, **1011**(1), 012009, 2018.